Low cost microcontroller implementation of Takagi–Sugeno Fuzzy MPPT controller for photovoltaic systems

Case Study

M'hand Oubella
Ibn Zohr University,
ESTA, Electrical Engineering Department,
Laboratory of Engineering Sciences and Energy Management (LASIME),
ESTA, BP: S33 – 80150, Agadir, Morocco
m.oubella@uiz.ac.ma

Mohamed Ajaamoum
Ibn Zohr University,
ESTA, Electrical Engineering Department,
Laboratory of Engineering Sciences and Energy Management (LASIME),
ESTA, BP: S33 – 80150, Agadir, Morocco
m.ajaamoum@uiz.ac.ma

Brahim Bouachrine
Ibn Zohr University,
ESTA, Electrical Engineering Department,
Laboratory of Engineering Sciences and Energy Management (LASIME),
ESTG, BP: S1317 – 81000, Guelmim, Morocco
b.bouachrine@uiz.ac.ma

Abstract *– Maximum power point trackers have a significant role in optimizing the energy conversion efficiency in a photovoltaic system. The numeric achievements of MPPT algorithm can be implemented and tested by using several embedded boards as Digital Signal Processor, Field-Programmable Gate Array, Arduino, and dspace. Alternatively, for the low cost, availability and simplicity, the PIC microcontrollers can be used compared with the other hardware devices. Therefore, this paper presents the implementation of a Takagi–Sugeno fuzzy controller on a low cost PIC microcontroller, for tracking the maximum power point of a PV module. The PV system consists of a PV emulator, DC-DC converter, and resistive load. The different steps in design, simulation and realization of the T-S Fuzzy logic controller are discussed. The proposed controller system was evaluated by comparing its performance metrics, in terms of efficiency and the Integral Square Error, with existing technique in the literature. The results corresponding to the experimental validation show that the proposed MPPT controller is able to ensure a perfect tracking of the maximum power point with variation of irradiance and is performing better than reported in a previous work.*

Keywords*: Photovoltaic, MPPT, Fuzzy Logic, Takagi–Sugeno, PIC16F877*

1. INTRODUCTION

For the past decades, the maximum power point tracking (MPPT) technique, in photovoltaic (PV) systems, has received a lot of attention in order to optimize the performance in these systems. The maximum power point (MPP) is not static; rather, it varies according to changes in atmospheric conditions. Therefore, MPPT is adopted to track and maintain the optimal operating condition of PV system, regardless of changing environment conditions [1]. MPPT techniques are most commonly applied in the DC-DC converters, which are used in photovoltaic systems as the MPPT circuit. The performance parameters of the PV system depend on both these converters and the MPPT algorithms. Many MPPT algorithms have been developed and implemented by different researchers [2], [3] and have offered various explanations for the problems associated with the MPPT controller. Recently, several comparative studies, of these algorithms, have been carried out in [4]–[6], where the MPPT algorithms are

categorized based on three main features: complexity, performance, and cost of implementation.

In literature, the conventional MPPTs are mostly used due to their ease of implementation. Among these MPPTs are Perturb and Observe [7], Hill Climbing [8], and Incremental Conductance [9]. Nevertheless, the main drawback of these algorithms is the power oscillation in the vicinity of the MPP, which leads to power loss and increases convergence time of the algorithm [4].

Several modern methods based on artificial intelligence have been proposed to remedy these issues, such as Artificial Neural Networks [10], and fuzzy logic controller (FLC) based *Mamdani or Takagi-Sugeno* model [11], [12]. These methods are accurate and efficient compared to the conventional techniques. Moreover, they respond quickly to changing environmental conditions and does not requiring any information of the PV model [4]. In order to design an accurate system, FLC uses knowledge and experience to construct the fuzzy rules base.

The achievement of MPPT algorithm can be implemented and tested by using microcontrollers [13], or embedded boards such as Digital Signal Processor [14], Field-Programmable Gate Array FPGA [15], Arduino [16], dSPACE [17]. For the implementation of MPPT algorithms, a proposal of the most appropriate embedded board was presented and discussed in [18]; the study was only focused on the low-cost electronic board. However, authors did not mention the cost-effective PIC microcontroller. Therefore, in this paper, we aim to contribute to the design and implementation of T-S fuzzy logic MPPT controller for a PV system on low cost microcontroller of type PIC 16F877. The hardware implementation of the MPPT algorithm based T-S Fuzzy Logic is carried out and the experimental prototype is tested for the PV system. The performance of the proposed controller is compared with the previously reported technique in the literature.

The remaining sections are organized as follows: in section 2, the investigation of PV system is presented. The section 3 is reserved to present the MPPT controller. Section 4 is devoted to hardware design and software implementation. Then, section 5 presents the experimental results and discussion on the effectiveness of the proposed MPPT controller. Finally, the conclusions are drawn in section 6.

2. PHOTOVOLTAIC SYSTEM AND MPPT CONTROLLER

Fig. 1 shows the system configuration used in this paper. This system is made up of a PV generator (PVG), current and voltage sensors, a DC-DC buck-boost converter, and a resistive load. Once voltage and current of the PV module are measured, they are sent to the control system, in which the algorithms are embedded. The duty cycle value of the buck-boost converter is adjusted by the MPPT based on T-S FLC and amplified by a driver circuit to get maximum power.

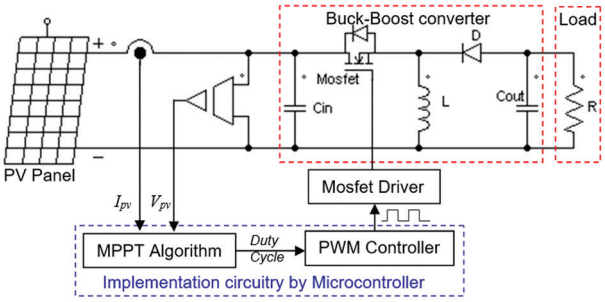

Fig. 1. Circuit diagram of PV system with MPPT based on T-S Fuzzy controller

2.1 PV PANEL MODEL

The PV panel is composed of several PV cells connected in series or parallel or both. The equivalent circuit of the single-diode model for PV cells is shown in Fig. 2. By neglecting the voltage drop in the series resistance of the generator and the current in the shunt resistor, the commonly used expression of the output current I_{PV} and output voltage V_{PV} of a PV panel with N_S cells in series and N_p strings in parallel [19] is:

$$I_{pv} = N_p\left(I_{ph} - I_0\left(exp\left(\frac{V_{pv}}{N_s V_T}\right) - 1\right)\right) \quad (1)$$

Where: I_{ph}, I_0 and V_T denote respectively the photocurrent, the reverse saturation current of the diode and the thermal voltage.

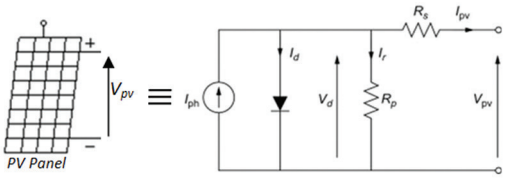

Fig. 2. Equivalent circuit for PV cell

In this work, a didactic bench emulating a solar module "CO3208-1A" (Fig. 3) is employed to simulate a PVG [20]. This bench consists of three independent blocks emulating solar panels; each with adjustable irradiance and integrated voltage and current displays.

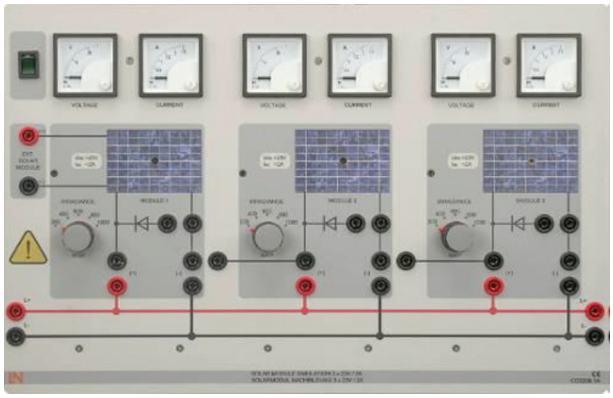

Fig. 3. "CO3208-1A" didactic bench emulating a solar module [20]

The key specifications of each block of this module are shown in table 1 under standard test conditions (STC), i.e., 25 °C and 1000W/m².

Table 1. The specifications of the solar module [20]

Model Parameters	Specification CO3208-1A
Open circuit voltage (V_{oc})	23V
Short circuit current (I_{sc})	2A
Maximum power (P_{mpp})	38W
Voltage at maximum power (V_{mpp})	21V
Current at maximum power (I_{mpp})	2A

Electrical characteristics of PV module Current-Voltage (I-V) and Power-Voltage (P-V) are illustrated by Fig. 4. It is very clear that these characteristics have non linear behavior with a single point where the PV power is maximum. This point varies with irradiation. Therefore, it is crucial to control DC-DC converter switch periodically via MPPT controller to have optimal energy of PV panel.

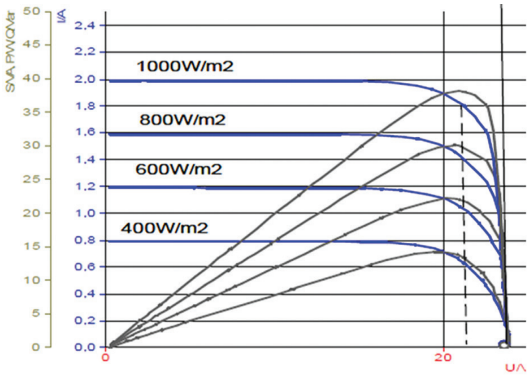

Fig. 4. The characteristics I-V and P-V of the solar module "CO3208-1A" [20]

2. 2 BUCK-BOOST CONVERTER

Buck-Boost converter, shown in Fig. 1, is chosen in the present work for matching the characteristics of the load with those of the PV panel. This converter is controlled using a Pulse-Width Method (PWM) and the duty cycle α is calculated for tracking the MPP of the PV panel.

The Buck-Boost converter can operate as Buck (for voltage step down) or Boost (for voltage step up) converter. However, the output voltage has the opposite sign to the input voltage. There are two operating modes for the buck-boost converter, namely, the continuous conduction mode (CCM) and the discontinuous conduction mode (DCM). Equations (2) to (4) are used to modeling buck-Boost converter in Continuous Conduction Mode.

$$\alpha = \frac{V_{out}}{V_{in} + V_{out}} \tag{2}$$

$$L = \frac{V_{in}.\alpha}{f_s.\Delta I_L} \tag{3}$$

$$C = \frac{V_{out}.\alpha}{f_s.\Delta V_{out}.R} \tag{4}$$

Where V_{in} is the input voltage, V_{out} is the output voltage and α is the duty ratio determined by the applied MPPT algorithm to directly control the converter switching. Δi_L is the current ripple, L is the inductance, ΔV_{out} is the output voltage ripple, C is the output capacitor, R is the load resistance, and f_s is the switching frequency.

2. 3 MAXIMUM POWER POINT TRACKING

According to the P-V characteristic of the PV panel shown in Fig. 4, the maximum power is produced for a particular voltage condition that depends on solar irradiation and temperature. Consequently, the MPP changes by moving on the PV curve depending on the weather conditions. As a result, an MPPT technique is needed so that the produced energy is always maintained at its maximum.

The PV panel produces a power expressed as follows: $P_{pv} = I_{pv}.V_{pv}$, hence:

$$P_{pv} = N_p\left(I_{ph} - I_0\left(exp\left(\frac{V_{pv}}{N_s V_T}\right) - 1\right)\right)\cdot V_{pv} \tag{5}$$

The condition which must be satisfied for the maximum power point PPM is:

$$\frac{dP_{pv}}{dV_{pv}} = 0 \tag{6}$$

$$\frac{dP_{pv}}{dV_{pv}} = I_{pv} - V_{pv}\frac{N_P.I_0}{N_s.V_T}exp\left(\frac{V_{pv}}{N_s V_T}\right) \tag{7}$$

The nonlinearity of equation (7) makes MPPT search difficult, so it is not easy to come by the MPPT using traditional methods. Thus, we will use the T-S fuzzy method to find the maximum power point.

3. MPPT T-S FUZZY CONTROLLER

3.1 CONCEPT OF MPPT FUZZY LOGIC CONTROLLER

The power–voltage characteristic illustrated in Fig. 5 shows that the variation of the maximum power (P_{MPP}) of PVG, which corresponds to an optimal PV output voltage (V_{MPP}), can be changed as a function of the solar irradiation and cell temperature. We introduce the concept of MPPT FLC as follows: The output power of PVG is examined by the FLC in each sample time (t) and then defines the change in power with respect to voltage (dp_{pv}/dv_{pv}). If this value is bigger than zero, the controller modifies the duty cycle $\Delta\alpha$ of PWM signal controlling the DC-DC converter to increase the voltage until the power is maximum ($dp_{pv}/dv_{pv} = 0$). If the value (dp_{pv}/dv_{pv}) is lower than zero the controller changes the duty cycle Δα to reduce the voltage until the power is maximized and so on. Fig. 5 illustrates this concept.

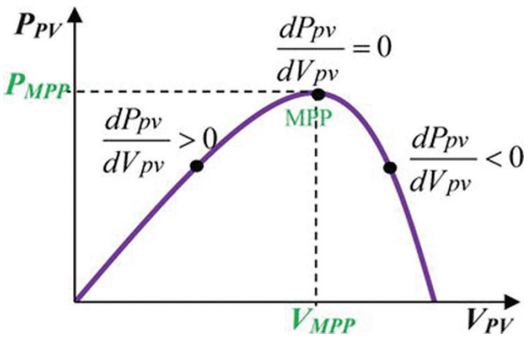

Fig. 5. The concept of MPPT fuzzy logic controller

3.2 THE PROPOSED STRUCTURE OF THE T-S FUZZY CONTROLLER

Two types of Fuzzy Inference Systems (FIS), *Mamdani and Takagi-Sugeno* are used in control applications. The *Takagi and Sugeno* (T-S) fuzzy model can be reformulated as a fuzzy dynamic model to represent nonlinear dynamic systems [21]. This fuzzy modelling method provides an alternative approach to describing complex nonlinear systems, compared with *Mamdani* fuzzy model; T-S fuzzy model can reduce the number of rules in modeling higher-order nonlinear systems [22]. The two models differ in compilation of output. The consequence parts of the *Mamdani* fuzzy model are fuzzy sets while those of the T-S fuzzy model are linear functions of input variables. In this paper, maximum power point tracking is implemented using a T-S fuzzy controller.

The principal operating of T-S Fuzzy inference systems is shown in Fig. 6.

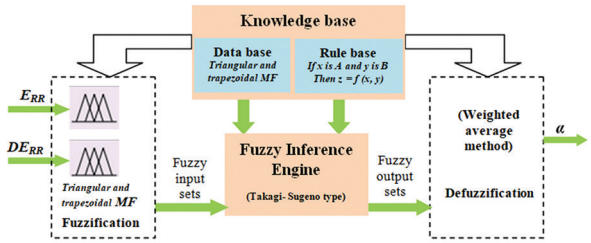

Fig. 6. T-S fuzzy model schema diagram principle

The fuzzy inference system contains five functional components:

- A fuzzification interface is used to convert crisp inputs (E_{RR} and DE_{RR}) to linguistic variables as fuzzy inputs applying membership functions (*MF*).
- A database is used to define membership functions.
- A rule base contains several fuzzy if-then rules.

The T-S style fuzzy rule is: *IF x is A AND y is B THEN z is f (x, y)* where *x, y* and z are linguistic variables, *A* and *B* are fuzzy sets on universe of discourses *X* and *Y*, and *f (x, y)* is a mathematical function.

- The inference engine of the FLC is a decision-making unit.
- The defuzzification interface is used to convert fuzzy outputs into crisp outputs.

The structure of the proposed T-S fuzzy controller is characterized by:

- The error E_{RR} (t) and change in error DE_{RR} (t) inputs, at sampled times t, are calculated by:

$$E_{RR}(t) = \frac{\Delta P_{pv}}{\Delta V_{pv}} = \frac{P_{pv}(t) - P_{pv}(t-1)}{V_{pv}(t) - V_{pv}(t-1)} \tag{8}$$

$$DE_{RR}(t) = E_{RR}(t) - E_{RR}(t-1) \tag{9}$$

- $P_{pv}(t)$ and $V_{pv}(t)$ are respectively the instantaneous power and voltage delivered by the PVG.

The membership functions for input error ERR are defined as:

$$\mu_i(NB) = Max\left(min\left(\left[\frac{-a_1 - E_{RR}}{-a_1 + a_2}\right], 1\right), 0\right) \tag{10}$$

$$\mu_i(NM) = Max\left(min\left(\left[\frac{E_{RR} + a_2}{-a_1 + a_2}\right], \frac{-E_{RR}}{a_1}\right), 0\right) \tag{11}$$

$$\mu_i(ZE) = Max\left(min\left(\left[\frac{E_{RR} + a_1}{a_1}\right], \left[\frac{a_1 - E_{RR}}{a_1}\right]\right), 0\right) \tag{12}$$

$$\mu_i(PM) = Max\left(min\left(\frac{E_{RR}}{a_1}, \left[\frac{a_2 - E_{RR}}{a_2 - a_1}\right]\right), 0\right) \tag{13}$$

$$\mu_i(PB) = Max\left(min\left(\left[\frac{E_{RR} - a_1}{a_2 - a_1}\right], 1\right), 0\right) \tag{14}$$

The change in error DERR membership functions is defined by the same Equations above (10 - 14) by changing a_1, a_2 and E_{RR} to b_1, b_2 and DE_{RR} respectively.

- The single output variable is the change in duty cycle $\Delta\alpha$ of PWM signal controlling the DC-DC converter.

$\Delta\alpha$ is defined by the control law, so that

$$\Delta\alpha(t) = (E_{RR}, DE_{RR})$$

The duty cycle α is defined as:

$$\alpha(t) = \alpha(t-1) + \Delta\alpha(t) \tag{15}$$

In the Takagi-Sugeno modeling, the final output is equal to the weighted average of the output of each rule. By using the Equation (16), we evaluate the net value $\Delta\alpha$ of the output variable, in which the summations are based on the 25 rules.

$$\Delta\alpha = \frac{\sum_{i=1}^{25} Z_i w_i}{\sum_{i=1}^{25} w_i} \tag{16}$$

With Z_i is the output level of each rule R_i and w_i is the degree of activation of each rule calculated by the following expression:

$$w_i = \mu_{E_{RRi}} \bullet \mu_{DE_{RRi}} \tag{17}$$

- The universe of discourse, which is normalized to the interval [-1, 1], is spitted into five fuzzy sets for input and output variables.

The triangular and trapezoidal membership functions are used in the proposed T-S fuzzy controller for inputs and singleton for output as well. Fig. 7 illustrates the appearance of these functions.

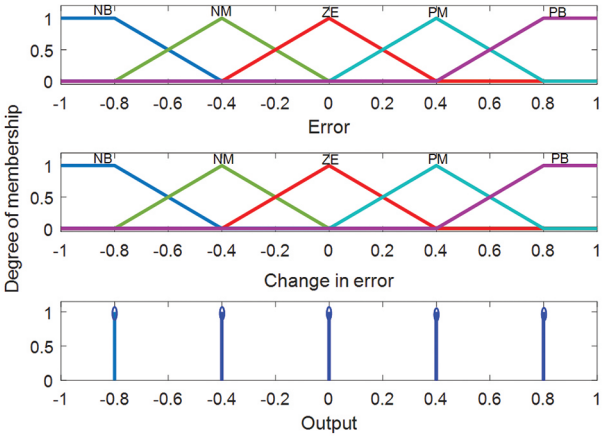

Fig. 7. Membership functions plots of the input variables (E_{RR}, DE_{RR}) and the output variable α

- Base of 25 rules.

We named the five fuzzy sets as follows: NB for negative big, NM for negative medium, ZE for about zero, PM for positive medium, and PB for positive big. Table 2 summarizes the basis of rules, which includes the 25 rules.

The flowchart in Fig. 8 graphically describes the steps of the algorithm required to generate a control signal on an output of the microcontroller. The output signal is connected to the MOSFET gate driver of the Buck-Boost converter.

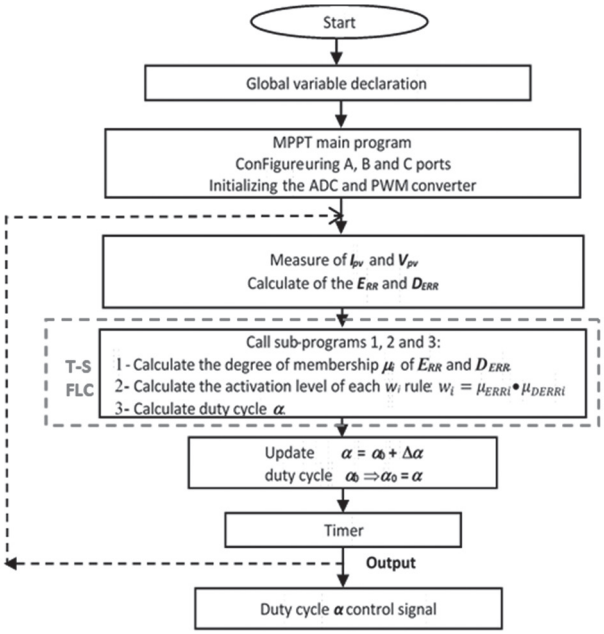

Fig. 8. Flowchart of MPPT algorithm based T-S Fuzzy logic

Table 2. Base of fuzzy rules

ERR / DERR	NB	NM	ZE	PM	PB
NB	PB	PB	PB	PM	ZE
NM	PB	PB	PM	ZE	NM
ZE	PB	PS	ZE	NM	NB
PM	PM	ZE	NM	NB	NB
PB	ZE	NM	NB	NB	NB

4. HARDWARE DESIGN AND SOFTWARE IMPLEMENTATION

This section offers details of the hardware components and the operation used in the experimental prototyping platform along with the software implementation. For the convenience of demonstration, we divided the section into two parts: software implementation and hardware description.

4.1. SOFTWARE IMPLEMENTATION OF MPPT ALGORITHM BASED T-S FUZZY LOGIC CONTROLLER

We translated the flowchart (Fig. 8) into a program implemented in the PIC 16F877 microcontroller through C-code. After several tests, we came up with a version of the program, which consists of three subprograms that describe the T-S Fuzzy Controller as illustrated in Fig. 8. These subprograms are detailed below.

First Sub-Program: The first sub-program, aims to calculate the degree of membership μ_i of the E_{RR} and DE_{RR}, for the five fuzzy classes used. The membership functions are calculated through the block diagram realized under Simulink (Fig. 9), which makes it easier to understand the program written in C language.

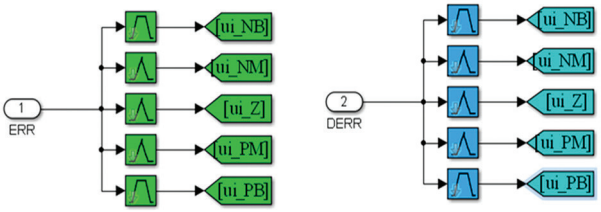

Fig. 9. Simulink model for fuzzification process

For the calculations of Equation (10) to (14), we are required to create *MAX* and *MIN* functions used to determine the degrees of membership for E_{RR} and DE_{RR} inputs, because the functions available for the PIC 16F877 microcontroller use integers (*Int*) and we use real numbers (*float*).

Second Sub-Program: With reference to Fig. 7 and based on the aforementioned universe of discourse, the purpose of this subprogram is to calculate the activation level w_i of each rule, using Simulink block diagram (Fig. 10).

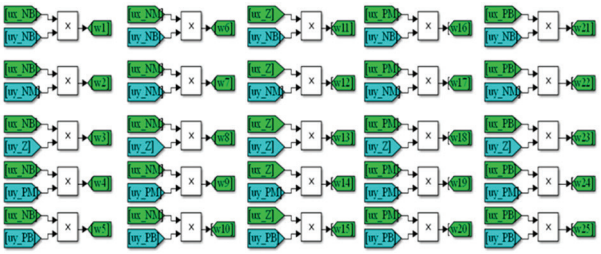

Fig. 10. Simulink model of the fuzzy rules

Third Sub-Program: After the rules application, a defuzzifier with the weighted average method is applied to adjust and generate the output analog signal. Thus, the call of the last sub-program allows calculating the new value of the duty cycle α that controls the switch of the Buck-Boost converter. Fig. 11 shows the blocks-set which achieve the expression of equations (15) and (16).

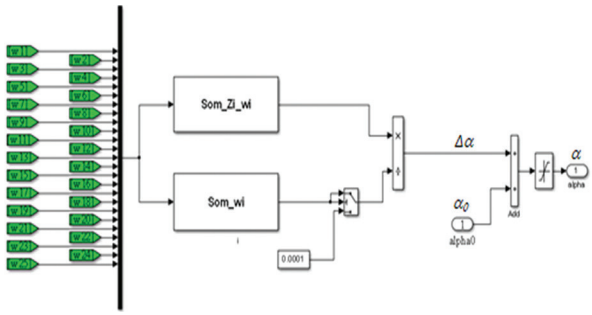

Fig. 11. Simulink model for defuzzification process

After obtaining satisfactory simulation results in MATLAB/Simulink, the Proteus 7 professional software was used for schematics drawing, circuits simulation and printed circuit board design. This software provides in its libraries electronic boards and microcontrollers such as PIC and Arduino. The PIC16F877 requires loading with a *HEX* file, through the use of the software tool MicroC PRO for PIC from Mikroelektronika. The schematic circuit of the embedded board developed for PIC16F877 is displayed in Fig. 12.

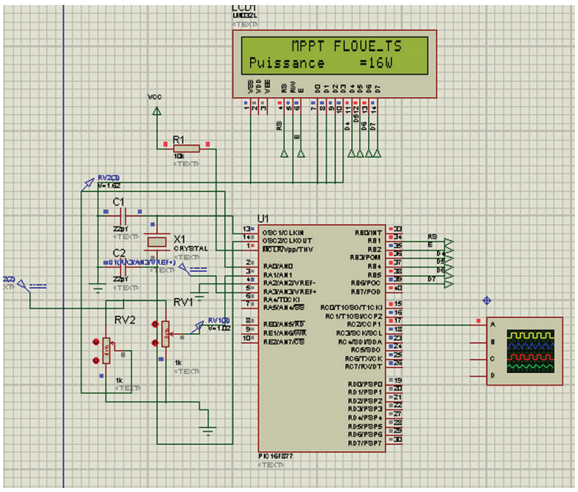

Fig. 12. Proteus schematic circuit developed using PIC16F877 Microcontroller

4. 2. HARDWARE DESCRIPTION

Fig. 13 below shows the block diagram of the hardware used for the experimentation corresponding to the photovoltaic system under study. It is composed of a PV emulator used as a power source, a Buck-Boost converter, I_{pv} and V_{pv} electrical sensors, and a resistive load. The PIC16F877 microcontroller is used to implement the proposed T-S Fuzzy algorithm.

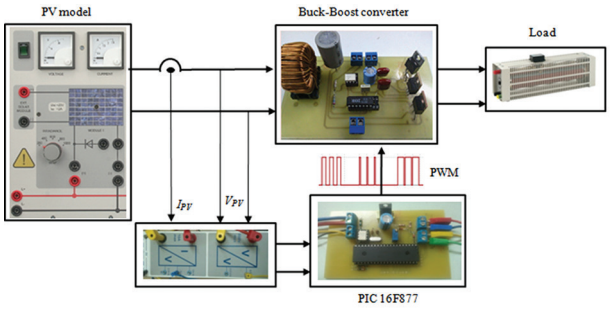

Fig. 13. Hardware implementation of the proposed T-S Fuzzy controller

The basic hardware components of the building blocks we used are included in the following sub-sections.

- *Buck-Boost converter*

The DC-DC converter is the main element of the PV system. It is an impedance matching circuit between the PVG and its load. A prototype of Buck-Boost converter shown in Fig. 14 is successfully developed to operate in the continuous current mode (CCM), according to the design steps developed in [23]. It is composed of a power MOSFET switch (IRF540), a Schottky diode (MBR20H), an inductor (2.75mH) and electrolytic filter capacitor (470µF) at the output side. The values of filter elements are calculated for the switching frequency of 15 KHz.

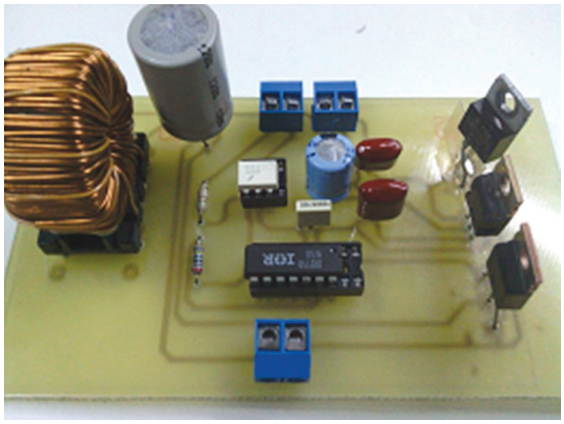

Fig. 14. Practical realization of the Buck-Boost converter.

The MOSFET transistor is controlled by a PWM signal generated from the MPPT control through an isolated Mosfet gate driver (IR2111) using simple optocoupler. The gate driver circuit is used to translate the voltage level of the PWM signal.

- *Current and voltage Sensors*

Fig. 15 illustrates a block used for measuring the current and voltage of the solar module. The block is equipped with a current sensor, based on a Hall-effect cell, and a voltage sensor; it consists of a model that incorporates sensors with the conditioning modules, which are arranged in an accessible form by printed connection terminals.

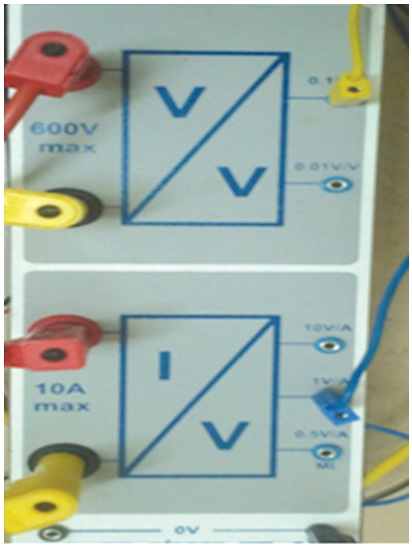

Fig. 15. The picture of the Current and voltage Sensors block.

The analogue outputs of sensors are given to on-chip Analog to Digital Converter (ADC) of the PIC16F877 microcontroller, which converts each analogue voltage to a decimal number thanks to the 10 bits resolution of the input ADC.

- *The PIC18F16778 Microcontroller Board*

Microcontroller is the common option of implementing the MPPT algorithm. The microcontroller selected, for our application, is PIC16F877 from Microchip Technology due to the availability of the device for the prototype. It is an 8-bit, 40-pins dual inline package (DIP). Table 3 describes key features of PIC16F877, which we used in this study.

Table 3. Key Features of the PIC16F877

Key Features	PIC16F877
Operating Frequency	20 MHz
Resets	POR, BOR
Flash Program Memory	8 K
Data Memory	368
EEPROM Data Memory	256
Interrupts	14
I/O Ports	Ports A,B,C,D,E
Timers	3
Capture/Compare/PWM modules	2
Serial Communication	USART
Parallel Communication	PSP
10 bit A/D module	8 input channels
Instruction set	35 instructions

Fig. 16 shows the embedded board developed for the PIC16F877, which represents the brain of the MPPT controller. It was designed and assembled using electronic circuits for programming. To generate the clock signal of the microcontroller, a 20 MHz crystal oscillator was used. The power supply of microcontroller board is considered basic and is, therefore, not discussed in this paper.

The microcontroller operation depends on the code that already programmed and uploaded into the board by using the software tool MicroC PRO for PIC, which provides a very efficient and advanced IDE (Integrated Development Environment).

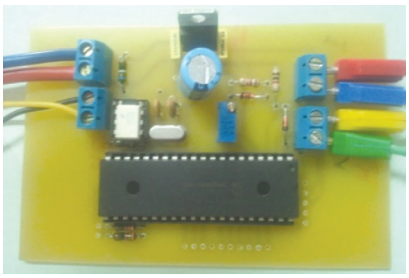

Fig. 16. The development board based on the PIC16F877 microcontroller

The output PWM signal is a square waveform with an amplitude value of 5 V at steady frequency of 15 kHz, and a variable duty cycle α based on the MPPT algorithm. The PWM signal feeds the MOSFET switch in the converter through the MOSFET driver.

5. EXPERIMENTAL RESULTS AND DISCUSSION

5.1. POWER–VOLTAGE CHARACTERISTIC OF THE MPPT BASED T-S FUZZY ALGORITHM

In this subsection, we consider the tracking performances under STC. To determine the system performance, we adopted three distinctive levels of irradiance G (600 W/m^2, 800 W/m^2 and 1000 W/m^2).

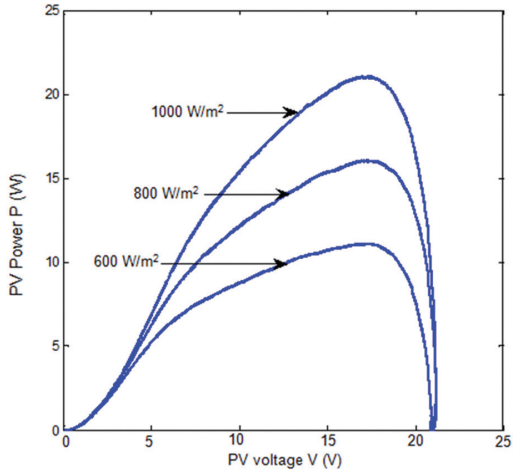

Fig. 17. P_{pv} (V_{pv}) characteristic of the Solar Module for different irradiation

Before launching the T-S MPPT controller, it is first necessary to carry out the plot of the static characteristic P_{pv} (V_{pv}), as a function of irradiation G, of the solar module used in this study. This characteristic is obtained using the block diagram of the hardware shown in Fig. 13 and the Matlab/Simulink environment. The Experimental P_{pv} (V_{pv}) characteristic (Fig.17) is provided to validate the performance of the proposed MPPT controller implemented on the PIC microcontroller.

Fig. 18 shows the experimental results of the MPPT tracking operation for different irradiations. We noticed that, due to the T-S Fuzzy MPPT algorithm implemented on PIC microcontroller, the MPP is reached with very little oscillations. These oscillations are occurred at the vicinity of MPP leading to power losses, which are almost neglected [4]. Hence, the proposed MPPT controller "T-S Fuzzy" is able to ensure a perfect tracking of the PPM of a solar module under variable irradiance.

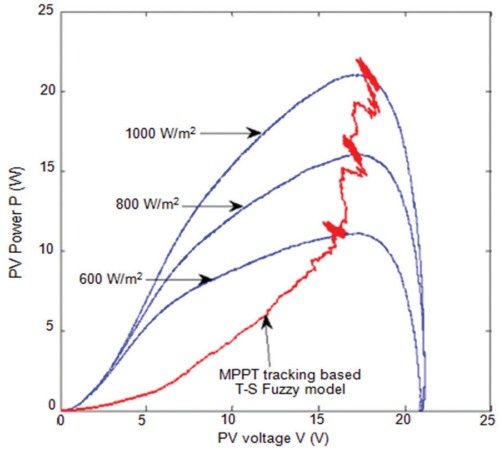

Fig. 18. MPPT tracking for different irradiation

The Tests of the MPPT controller "T-S Fuzzy", implemented on PIC microcontroller, are realized in static and dynamic conditions. Fig. 19 depicts the PV power for T-S Fuzzy MPPT technique for step-change in the irradiance from 600W/m² to 1000W/m².

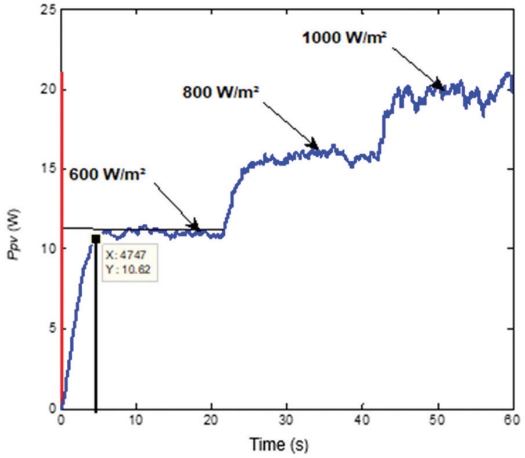

Fig. 19. Output power versus time under T=25 °C and step increasing of irradiance G

According Fig. 19, the respective maximum values of output power were 11.01, 16.13 and 20.35 W. These values are extremely close to the maximum values of the PV module as deduced from the experimental P_{pv} (V_{pv}) characteristics (Fig. 18).

Moreover, for the dynamics of the MPPT controller, it is noted from Fig. 19 that the output power reaches 96% of the MPP corresponding to G = 600 W/m² in 4.47 s. Based on these findings, we conclude that the proposed T-S Fuzzy MPPT controller achieves the correct tracking of the MPP, consequently proving its good performance in terms of finding the MPP under sudden changes in solar irradiation.

5.2. PERFORMANCES OF THE T-S FUZZY MPPT CONTROLLER IMPLEMENTED ON PIC MICROCONTROLLER

- *Comparison of Output Power of Solar Module with and without MPPT:*

A comparison is done between the output power with the MPPT circuit and without the MPPT circuit. The load here is taken to be the same for both circuits that is 30 Ω.

In Table 4, the efficiencies of the Photovoltaic System are compared with and without the MPPT. The Table displays the output power at load and the maximum power that can be delivered by the solar module under different irradiance.

Table 4. Comparison of output power of solar module without and with MPPT based T-S Fuzzy

Irradiance G (W/m²)	P_{pv} at load without MPPT (W)	P_{pv} at load with MPPT based T-S Fuzzy (W)	Efficiency (η)	Efficiency (%)
600	10.92	11.01	0.09	0.8
800	11.71	16.13	4.42	37.74
1000	12.87	20.35	7.48	58.11

Based on the results presented in Table 4 and for the developed MPPT T-S Fuzzy controller, the PV output power achieves the values 11.01, 16.13 and 20.35W, for the respective G values of 600, 800 and 1000 W/m². This presents almost 100% of the maximum power that the solar module can provide under the same experimental conditions. Comparing these results with those we found without of the presence of an MPPT controller, we conclude that the MPPT T-S Fuzzy controller contributed to a power gain of up to 58%, in the case of G =1000 W/m².

- *Performance criteria*

The experimental evaluation of the MPPT controller performances, implemented on PIC microcontroller, is presented by two performance criteria.

- The performance criterion η_{MPPT}, which characterizes the efficiency of the MPPT controller, defined by Equation (18).
- The Integral of the Squared Error (ISE) criterion, which characterizes the speed of response of MPPT controller. This criteria is defined by Equation (19):

$$\eta_{MPPT} = \frac{\int_0^t P_{min}(t)dt}{\int_0^t P_{max}(t)dt} \quad (18)$$

$$ISE = \int_0^t \left[e(t)\right]^2 dt \quad (19)$$

The criteria η_{MPPT} and ISE are calculated by means of the Simulink block diagram as shown in Fig. 20 (*a*) and (*b*), which are developed from the Equations (16) and (17) respectively.

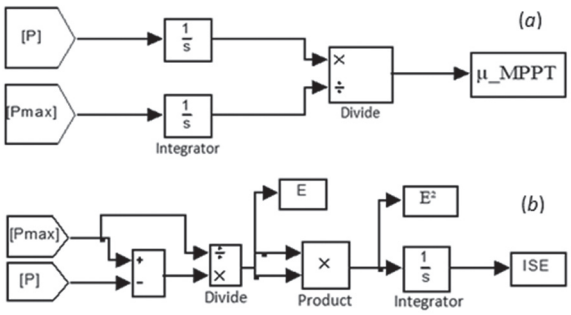

Fig. 20. Simulink model to determine: (*a*) Efficiency, (*b*) ISE.

Under the same experimental conditions that is for a step change of solar irradiance from 0 to 600W/m² and a period of 60s, we compare the performances of the two techniques used for the implementation of T-S Fuzzy MPPT controller; the rapid prototyping (T1) reported in [23] and the proposed technique (T2).

The results from comparing the criteria η_{MPPT} and ISE are presented in Figs. 21 and 22 respectively. The results of the proposed technique were obtained from the experimental measurements using the platform shown in Fig. 13, while those of the rapid prototyping are obtained from the experimental measurements using the PCI 1711 acquisition card [23].

As Fig. 21 shows, the curves associated with the two techniques are quite similar. However, we noticed that the T1 method tends to increase rapidly than T2. But, beyond 40 s, the trend is reversed, which enables reading the steady state faster with the proposed technique.

Under steady state condition, if the efficiency of an MPPT is greater than 97% then it is considered the best as reported in [24]. Hence, from the comparison of the η_{MPPT}, it follows that the proposed technique is quite effective, with its η_{MPPT} = 97.44% against η_{MPPT} = 96.32% for the rapid prototyping technique.

Under the same experimental conditions, Fig. 22 shows the "Integral of Squared Error" ISE curves determined for the two respective techniques T1 and T2. In this comparison, it is clear that the T2 technique is more efficient, with its ISE=1.28 lower than that of the T1 technique characterized by its ISE=1.44.

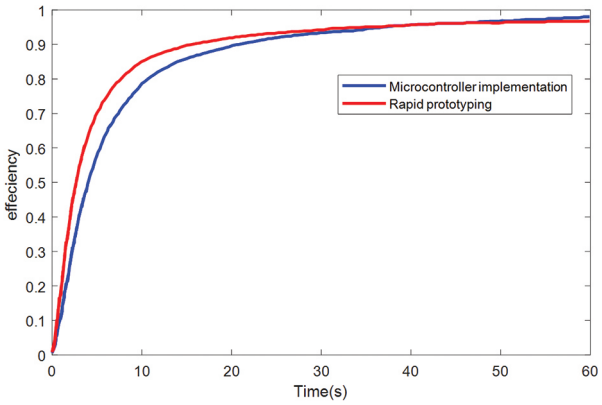

Fig. 21. η_{MPPT} criteria comparison

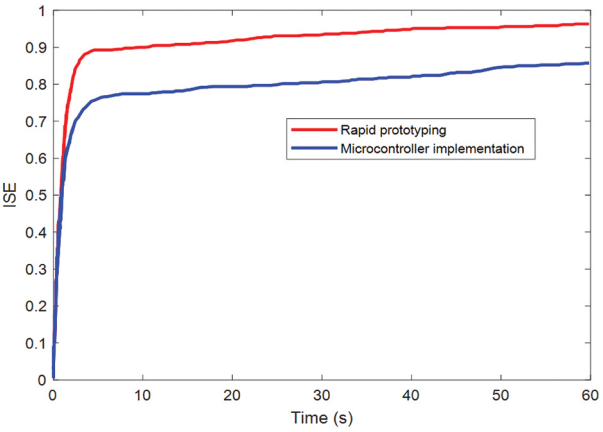

Fig. 22. ISE criteria comparison

Summary of the comparison between the two techniques

After presenting the results obtained by the realized T-S Fuzzy MPPT controller implemented on PIC microcontroller and compared with rapid prototyping reported in [23], we offer a summary of the results in Table 5. In this Table, we compared the two techniques based on three criteria: the efficiency η_{MPPT}, ISE Criteria and the response time.

Table 5. Comparison of parameters between rapid prototyping and implementation of MPPT "T-S Fuzzy" on PIC microcontroller

Technique	η_{MPPT} (%)	ISE	Response Time (s)
Rapid Prototyping [23]	96.32	1.44	2.39
Microcontroller implementation	97.44	1.28	4.74

Based on the results obtained in this work and the criteria previously cited, we can see that the proposed technique contributes to better results than the rapid prototyping in terms of efficiency and ISE criterion.

However, we notice that the response time of the proposed method is about two times greater than the rapid prototyping one. This difference is due to transient response of converter circuit and other circuitry. The low cost microcontroller as compared to the reported method compensates for this disadvantage, taking into account that the desired point to be reached in this system is obtaining the maximum yield from the PV panel.

6. CONCLUSION

This paper described the design of control strategy based on the *Takagi–Sugeno* fuzzy algorithm controller for the MPPT of a PV energy system. The T-S fuzzy algorithm has been successfully implemented in a low cost PIC 16F877 microcontroller. The proposed controller has been tested in a PV system consisting of a solar module, a Buck-Boost converter and a resistive load. Simulation and experimental results have been carried out to evaluate the effectiveness of the proposed controller system.

The results show that the MPPT controller "T-S Fuzzy" is able to ensure a perfect tracking of the PPM of a solar module under variable irradiance. The performance of the proposed controller is compared with the previously reported technique in the literature built around the PCI 1711 acquisition card in terms of efficiency and the Integral Square Error (ISE) index. The experimental results show the superiority of our T-S Fuzzy controller with η_{MPPT} = 97.44% against η_{MPPT} = 96.32% and ISE=1.28 lower than ISE=1.44 as compared with the existing techniques. Thus, the proposed controller based on low-cost microcontroller tends to perform better than controllers reported in previous work and can work properly for MPPT applications.

This work and the results presented herein, which can be used for PV energy harvesting as well, may be helpful for the design of the energy harvesting-based embedded systems. For further research, we intend to conduct a deeper experiment that corroborates our conclusions from this work by using more efficient MPPT algorithms to extract maximum power from PV system at real time.

7. REFERENCES

[1] M. A. Eltawil, Z. Zhao, "MPPT Techniques for Photovoltaic Applications", Renewable and Sustainable Energy Reviews, Vol. 25, 2013, pp. 793-813.

[2] Y. E. Abu Eldahab, N. H. Saad, A. Zekry, "Enhancing the maximum power point tracking techniques for photovoltaic systems", Renewable and Sustainable Energy Reviews, Vol. 40, 2014, pp. 505-514.

[3] M. S. Sivagamasundari, D. P. M. Mary, V. K. Velvizhi, "Maximum Power Point Tracking For Photovoltaic System by Perturb and Observe Method Using Buck Boost Converter", International Journal of Advanced Research in Electrical, Electronics and Instrumentation Engineering, Vol. 2, No. 6, 2013, p. 2433-2439.

[4] A. Gupta, Y. K. Chauhan, R. K. Pachauri, "A Comparative Investigation of Maximum Power Point Tracking Methods for Solar PV System", Solar Energy, Vol. 136, 2016, pp. 236-253.

[5] M. A. G. de Brito, L. Galotto, L. P. Sampaio, G. d. A. e Melo, C. A. Canesin, "Evaluation of the Main MPPT Techniques for Photovoltaic Applications", IEEE Transactions on Industrial Electronics, Vol. 60, No. 3, 2013, pp. 1156-1167.

[6] S. Motahhir, A. El Ghzizal, S. Sebti, A. Derouich, "MIL and SIL and PIL tests for MPPT algorithm", Cogent Engineering, Vol. 4, No. 1, 2017, p. 1378475.

[7] M. Abdel-Salam, M.T. El-Mohandes, M. Goda, "An Improved Perturb-and-Observe based MPPT Method for PV Systems under Varying Irradiation Levels", Solar Energy, Vol. 171, 2018, pp. 547-561.

[8] X. Xiao, X. Huang, Q. Kang, "A Hill-Climbing-Method-Based Maximum-Power-Point-Tracking Strategy for Direct-Drive Wave Energy Converters", IEEE Transactions on Industrial Electronics, Vol. 63, No. 1, 2016, pp. 257-267.

[9] R. I. Putri, S. Wibowo, M. Rifa'i, "Maximum Power Point Tracking for Photovoltaic Using Incremental Conductance Method", Proceedings of the 2nd International Conference on Sustainable Energy Engineering and Application, Bandung, Indonesia, 14-16 October 2014, pp. 22-30.

[10] M. Yaichi, M.K. Fellah, A. Mammeri, "A Neural Network Based MPPT Technique Controller for Photovoltaic Pumping System", International Journal of Power Electronics and Drive Systems, Vol. 4, No. 2, 2014, pp. 241-255.

[11] L. Suganthi, S. Iniyan, A. A. Samuel, "Applications of Fuzzy Logic in Renewable Energy Systems - A review", Renewable and Sustainable Energy Reviews, Vol. 48, 2015, pp. 585-607.

[12] M. Truntič, A. Hren, M. Milanovič, M. Rodič, "Adaptive Fuzzy-Logic State Controller for DC-DC Step-Down Converter", Electrical Engineering, Vol. 100, No. 2, 2018, pp. 983-995.

[13] B. R. S. Reddy, P. B. Narayana, P. Jambholkar, K. S. Reddy, "MPPT algorithm implementation for solar photovoltaic module using microcontroller", Proceedings of the Annual IEEE India Conference, Hyderabad, India, 16-18 December 2011, pp. 1-3.

[14] R. Akkaya, A. A. Kulaksız, Ö. Aydoğdu, "DSP Implementation of a PV System with GA-MLP-NN Based MPPT Controller Supplying BLDC Motor Drive", Energy Conversion and Management, Vol. 48, No. 1, 2007, pp. 210-218.

[15] A. Al-Gizi, B. Al-Rawe, M. Al-Saadi, A. Craciunescu, "Step by Step FPGA-Based Implementation of MPPT Fuzzy Controller for PV Systems", Proceedings of the 11th International Symposium on Advanced Topics in Electrical Engineering, Bucharest, Romania, 28-30 Mar. 2019, pp. 1-6.

[16] A. Al-gizi, M. Al-saadi, S. Al-chlaihawi, A. Craciunescu, M. A. Fadel, "Experimental Installation of Photovoltaic MPPT Controller Using Arduino Board", Proceedings of the International Conference on Applied and Theoretical Electricity, Craiova, Romania, 4-6 October 2018, pp. 1-6.

[17] O. F. Kececioglu, A. Gani, M. Sekkeli, "Design and Hardware Implementation Based on Hybrid Structure for MPPT of PV System Using an Interval Type-2 TSK Fuzzy Logic Controller", Energies, Vol. 13, No. 7, 2020, p. 1842.

[18] S. Motahhir, A. El Hammoumi, A. El ghzizal, "The Most Used MPPT Algorithms: Review and the Suitable Low-cost Embedded Board for Each Algorithm", Journal of Cleaner Production, Vol. 246, 2019, p. 118983.

[19] H. Abid, F. Tadeo, M. Souissi, "Maximum Power Point Tracking for Photovoltaic Panel based on T-S Fuzzy Systems", International Journal of Computer Applications, Vol. 44, No.22, 2012, pp. 50-58.

[20] L. Nülle, EPH 2.1 Investigating solar modules. https://www.lucas-nuelle.com/316/apg/13223/EPH-2.1-Investigating-solar-modules.htm (accessed: 2021)

[21] S. G. Cao, N. W. Rees, G. Feng, "Analysis and Design for a Class of Complex control Systems Part I: Fuzzy Modelling and Identification", Automatica, Vol. 33, No. 6, 1997, pp.1017-1028.

[22] M. Sugeno, "On Stability of Fuzzy Systems Expressed by Fuzzy Rules with Singleton Consequents", IEEE Transactions on Fuzzy Systems, Vol. 7, No. 2, 1999, pp. 201-224.

[23] M. Ajaamoum, M. Kourchi, B. Bouachrine, M. Oubella, A. Ihlal, L. Bouhouch, "Rapid Prototyping Test Bed of MPPT Photovoltaic Controller Based on Takagi-Sugeno Fuzzy Models", IREMOS, Vol. 12, No. 5, 2019, p. 303-312.

[24] R. Ahmad, A. F. Murtaza, H. A. Sher, "Power Tracking Techniques for Efficient Operation of Photovoltaic Array in Solar Applications - A review", Renewable and Sustainable Energy Reviews, Vol. 101, 2019, pp. 82-102.